Geophys. J. R. astr. Soc. (1984) **78**, 751–773

Palaeomagnetism of some late Mesozoic dolerite sills of East Central Spitsbergen, Svalbard Archipelago

S. A. Vincenz, M. Jeleńska* and K. Aiinehsazian
Department of Earth and Atmospheric Sciences, Saint Louis University, PO Box 8099–Laclede Station, Saint Louis, Missouri 63156, USA
K. Birkenmajer *Institute of Geology, Polish Academy of Sciences, Cracow, Poland*

Received 1984 February 21; in original form 1983 July 18

Summary. Two late Mesozoic dolerite sills, situated near Agardhbukta on the east coast of Vestspitsbergen and dated radiometrically at 100 ± 4 Myr BP, have been sampled in five localities and subjected to detailed mineralogical and rock magnetic studies to determine the direction and origin of their magnetization. Although the sills lie outside the Tertiary orogenic belt, one locality (no. 4) has undergone strong hydrothermal alteration and a small part of another locality (no. 3) has also been affected. A conventional procedure based on examination of Zijderveld diagrams, applied to specimens demagnetized by alternating fields and thermally, yielded similar remanence directions at all five localities, except at the altered part of locality 3. Using a least squares computer method of analysis of step demagnetization data, comparable directions were isolated from all localities, including the altered part of locality 3. Except in this last case, all directions were reversed. The adjusted mean direction obtained from this analysis is $D = 159.0°$, $I = 62.2°$, $\alpha_{95} = 9.0°$ yielding a palaeomagnetic pole situated at 225.0°, 54.3°N comparable with pole positions obtained from other late Mesozoic igneous rocks on Spitsbergen and distinct from palaeopoles derived from Mesozoic rocks in North America and Eurasia. This suggests that during the late Mesozoic Svalbard existed as a semi-independent microplate.

1 Introduction

Most of the continental crust exposed on the edges of the Arctic Basin has been ice bound, and only a few areas remain, where the outcrops are accessible for palaeomagnetic sampling. Spitsbergen, the largest island of Svalbard Archipelago, is one of these areas and it has been

*On leave of absence from Institute of Geophysics, Polish Academy of Sciences, Pasteura 3, 00-973 Warsaw, Poland.

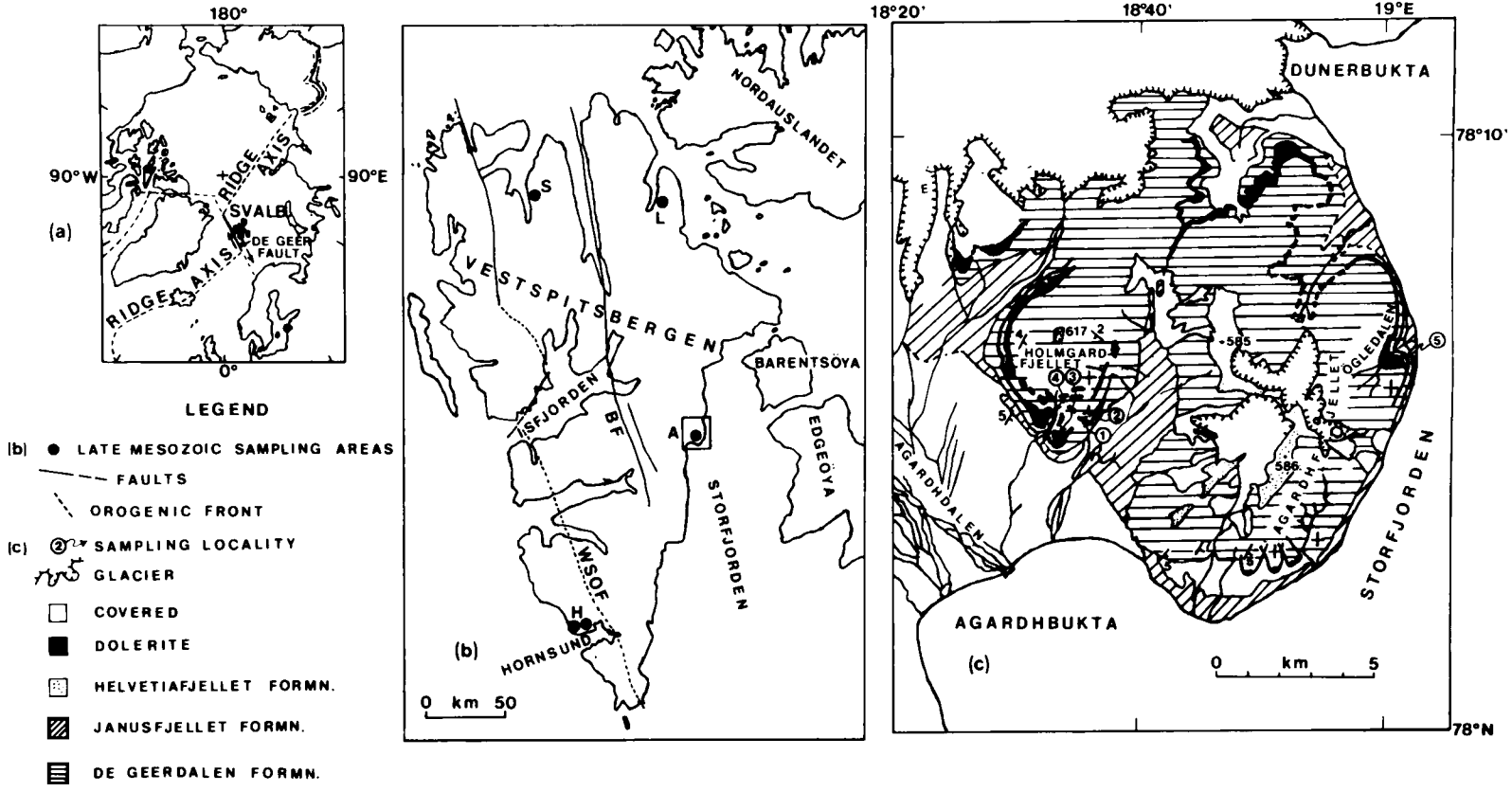

Figure 1. Sketch map of Svalbard. (a) Location of Svalbard in the Arctic Basin, (b) late Mesozoic sampling areas: A, Agardhbukta; L, Lomfjord sill; S, Sörlifjell volcano; H, Hornsund dykes. WSOF, West Spitsbergen orogenic front; BF, Billefjorden Fault. (c) Geological sketch map of Agardhalen sills, showing location of sampling localities.

subject of palaeomagnetic studies for the past decade or so (Fig. 1a). Recently, data derived from late Mesozoic dolerite dykes (Jeleńska *et al.* 1978–79; Vincenz *et al.* 1981) combined with information obtained from other units (Sandal & Halvorsen 1973; Briseid & Halvorsen 1974) gave a clear and significant indication of the behaviour of the Cretaceous geomagnetic field in the area, suggesting that Svalbard must have played a significant role in the formation of the Neo-Arctic Basin. Confirmation of these results using other Mesozoic dolerites appears of great importance and the present paper deals with palaeomagnetism of dolerite sills outcropping on the east coast of Spitsbergen.

This area was selected to obtain palaeomagnetic data from rock units situated outside the Tertiary orogenic belt, i.e. unaffected by the West Spitsbergen orogeny (Harland 1969; Birkenmajer 1972) (Fig. 1b).

2 Geology and sampling

The area investigated lies north of Agardhbukta and north-east of Agardhdalen on the east coast of Vestspitsbergen (Fig. 1b, c). The dolerites form sills with occasional dyke offshoots within the late Jurassic, possibly Oxfordian, marine shales of the Agardfjellet member (Janusfjellet Formation). Radiometric age determination carried out on dolerites of Holmgardfjellet gave an age of 100 ± 4 Myr BP (Burov *et al.* 1977), corresponding to the Albian–Cenomanian boundary on the stratigraphic scale. Two parallel sills are well exposed. At Holmgardfjellet the sills are almost horizontal and dip comformably with the Jurassic shale at 2–4° to the south-east. Here the lower sill was sampled at localities 1 and 4 and the upper sill at localities 2 and 3. At Ogledalen only the upper sill was sampled at locality 5 (Fig. 1c).

A total of 49 block samples was obtained, each from a different sampling site and in addition 11 cores drilled *in situ* were derived from two sites. Three hundred and nineteen cylindrical specimens were obtained from the block samples and cores. A Brunton compass or equivalent was used to orient the block samples and cores and care was taken to check for the effect of magnetization of rock face on the magnetic needle, but no such effect was observed. On average two to three cylindrical specimens were derived from each core drilled *in situ* and each block sample yielded eight to 10 specimens. Five block samples, each representing a locality and comprising 42 specimens, were set aside for the study of magnetic properties of the dolerites. This yielded a total of 46 sites comprising 277 specimens for palaeomagnetic studies.

3 Microscopic investigations

The petrographic characteristics of Spitsbergen dolerites have been described by Tyrell & Sandford (1933) and according to their classification the sills of Agardhbukta belong to type A of the four types, which comprises medium to fine grained slightly differentiated black olivine dolerite with a partly doleritic and partly ophitic structure and is typical for the greater part of sills and other intrusions on the island.

Microscopic studies of polished sections supported by transmitted light investigations showed that the magnetic material in rock at localities 1, 2 and 3 consisted of relatively little altered deuteric oxidation class 1 or seldom class 2 titanomagnetite (TM), while the dolerite of locality 5 belonged to class 2 or rarely 3 with an overprint of moderate hydrothermal alteration. The rock at locality 4 and part of locality 3 had undergone class 1 deuteric oxidation and was strongly altered, indicating an overprint of strong hydrothermal alteration. Deuteric (high temperature) oxidation classes of TM have been defined by Wilson & Watkins (1967), Wilson, Haggerty & Watkins (1968) and Ade-Hall *et al.* (1968). The TM

was frequently intergrown with primary ilmenite and accompanied by accessory pyrite or pyrrhotite which occurred here and there in the form of large grains with diameters ranging from 100 to 600 μm. Ilmenite was commonly unaltered and occurred in the form of laths (also 100–500 μm) or smaller rods and skeletal grains. TM grain diameters ranged in size from 1 to 500 μm with the larger grains (100–200 μm) predominating in localities 1 and 2, but generally two generations of grains occurred, smaller ones (1–10 μm) and larger grains (10–500 μm). Small grains were present as inclusions in the matrix, particularly in olivines and feldspars, while larger grains occurred as independent crystals. Some TM grains revealed submicroscopic anisotropy and discolouring, suggesting effects of low-temperature oxidation resulting from hydrothermal alteration. At localities 1, 2 and 5 this effect was also indicated by some granulation and incipient maghaemitization around the rims of some of the grains (locality 5). Strong hydrothermal alteration was found in samples from one part of the sill outcrop at locality 3 (designated 3A) and was widely spread at locality 4. In both cases this was indicated by very strong granulation of TM which was at times almost completely altered either to the point of strong maghaemitization/haematization or even total decomposition into iron carbonates. Very few unaltered TM grains were in fact present and some grains revealed large holes or cracks filled with non-opaque material. Small pyrite grains, accompanied by pyrrhotite, were observed in greater numbers then at other localities. Transmitted light studies established presence of secondary minerals such as prehnite and epidote and the silicate rock matrix revealed presence of red staining, observed using both reflected and transmitted light and indicating migration of iron cations out of the magnetic grains through the holes and cracks in these grains (Marshall & Cox 1972) and formation of new iron silicates. It has been shown conclusively that appearance of red staining in the silicates surrounding TM grains corresponds to stage 4 of low-temperature oxidation produced by hydrothermal alteration (Johnson & Melson 1977; Johnson & Hall 1978; Ryall & Hall 1980).

The above investigations were repeated on representative samples from all five localities after heating in air in the laboratory to 600°C. Discolouration and granulation of some TM grains observed in virgin samples of localities 1, 2 and 3 increased and red staining appeared in rock matrix, all these effects suggesting a continuing oxidation process. Generation of very fine magnetic material in olivine grains in the form of tiny pin-point spots was observed. All these effects became intensified in heated material from locality 5, where the TM grains became almost completely haematized and the increase in pseudomorphous red staining was also more pronounced. The symptoms of strong hydrothermal alteration at locality 4 were greatly enhanced by heating, resulting in total haematization of TM or replacement of iron oxides by fine grained aggregates of iron carbonates.

It is concluded from the above studies that the dolerite at locality 4 and part of locality 3 has different magnetic mineralogical characteristics from the dolerites at the other localities and that this will have to be taken into account in the interpretation of its palaeomagnetic make-up.

4 Magnetic properties of the dolerites

To identify the magnetic minerals which were carriers of the natural remanence (NRM) and determine its origin and age, a study of magnetic properties of the dolerites was carried out. This was necessary to provide evidence that the dolerites were suitable for palaeomagnetic studies, i.e. that palaeomagnetic directions obtained would reflect the direction of late Mesozoic geomagnetic field in which the dolerites were formed. To identify the carriers of the NRM, Curie point investigations were conducted using a conventional Curie balance and small rock chips or powdered magnetic material extracted from the various samples.

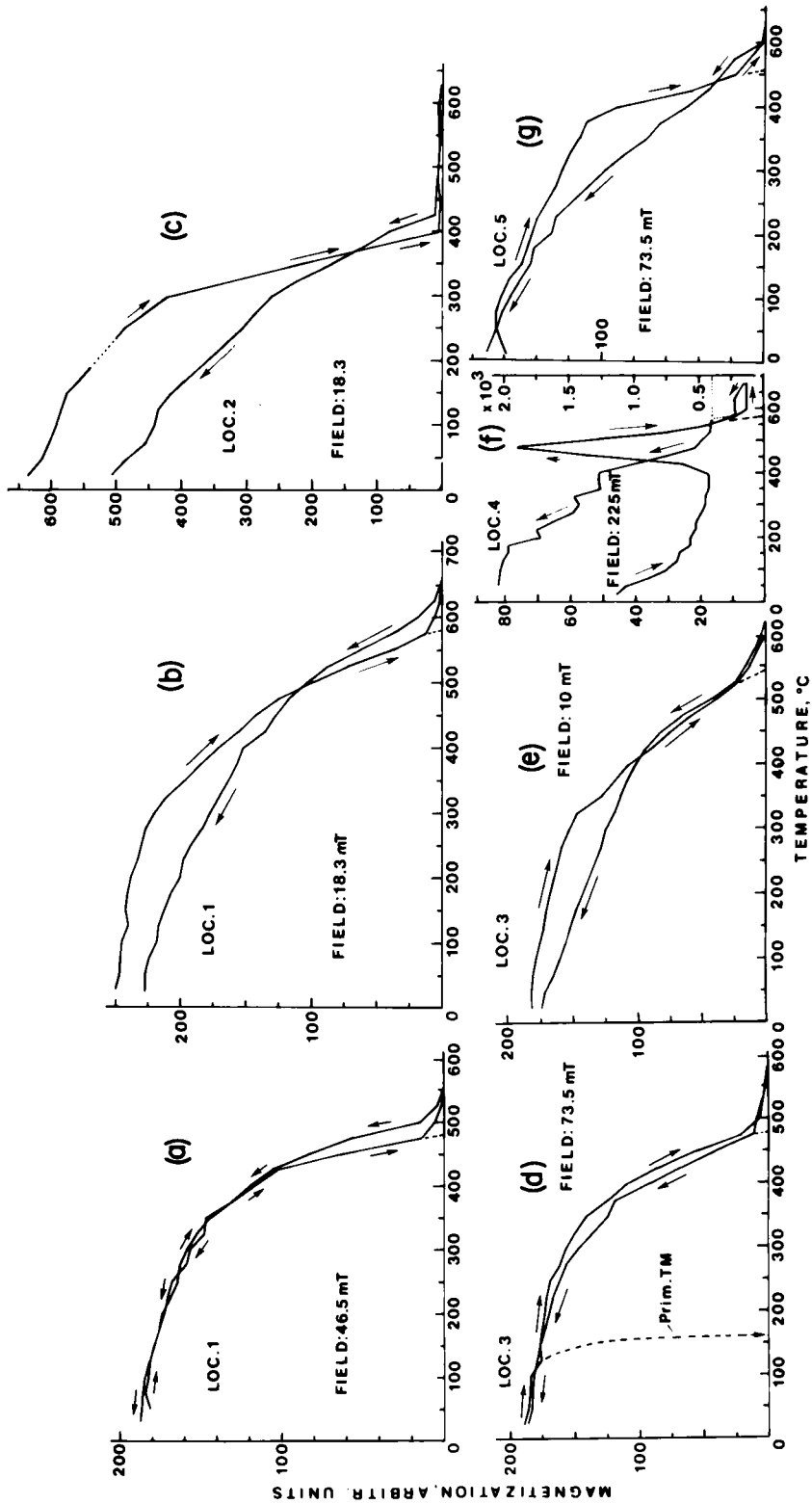

Figure 2. Determination of Curie temperatures: arrows pointing to the right and left indicate the heating and cooling curves respectively. Curve (f) for rock material from locality 4 reveals presence of oxidized pyrite/pyrrhotite which converts at higher temperatures to magnetite and/or maghaemite. The ordinate scale for the cooling curve is in this case given on the right side.

The results of these strong-field observations are summarized in Fig. 2, showing variation of saturation magnetization with temperature measured for representative material from five localities. The magnetizing field used ranged from 10 to 225 mT and though saturation was not achieved in all cases, the induced moments were nevertheless sufficiently close to saturation moments at room temperature to accept these measurements as representing the variation of saturation magnetization with temperature.

Presence of a relatively high Curie temperature phase of TM was established at all the localities (Fig. 2). The behaviour of the material from locality 4 suggests that, apart from the altered TM, this dolerite rock contains some magnetic pyrrhotite, in part in the form of very fine grains, possibly in a quasi-superparamagnetic state, as suggested by decrease of the moment already below 100°C (Fig. 2f). The Curie point of pyrrhotite is about 300–310°C (Schwarz 1967, 1968) and it oxidizes to magnetite and/or maghaemite at temperatures above 400°C (Schwarz 1975). Since heating was continued above 500°C, additional magnetite and/or maghaemite may have been formed by the mechanism of decomposition of olivine referred to in section 3 as well as by breakup of iron carbonates and part of the 20-fold increase of intensity (Fig. 2f) may also be due to these causes.

Isothermal remanent magnetization (IRM) was imposed stepwise on representative specimens from each locality until saturation was achieved and then was demagnetized by alternating magnetic field (AF demagnetization). These operations were repeated using thermal demagnetization and the results of these experiments are summarized in Fig. 3. It is evident that the dolerites magnetize easily and those from localities 1, 2 and 3 achieve over 95 per cent of saturation at 0.01 T and become fully saturated at 0.1 T. The material from locality 4 is, however, magnetically harder and saturation is not achieved below 0.25 T, while the dolerite from locality 5 still does not saturate at that field value.

The behaviour on AF demagnetization of the IRM shown by full circles is in full agreement with that exhibited on its acquisition. The slope of IRM acquisition curves depends on the size of magnetic grains and for TM is related to the fraction of its ulvöspinel content (Day 1977). Since the slopes in Fig. 3 are large, the experiments suggest that the dolerites at all five localities contain magnetic material consisting of relatively large (> 50 μm) multidomain (MD) grains (Soffel 1971).

The above conclusions can be considered in terms of median destructive fields which are easily deduced from Fig. 3. These are 4.5 mT for localities 1, 2 and 3, 8 mT for locality 4, and 17.5 mT for locality 5. These figures can be compared with the results obtained by Dankers (1981) for synthetic samples of magnetite and TM and in terms of his data the material in the rocks from localities 1, 2 and 3 is TM with grain sizes 30–40 μm, while the material from localities 4 and 5 would be magnetite with grain sizes 25–55 μm and less than 5 μm respectively.

The blocking temperatures of saturation IRM are distributed, but thermal demagnetization curves (shown by dashed lines in Fig. 3) reveal temperatures of disappearance of IRM in the range between 520 and 550°C for rock at localities 1, 2, 3 and 4 and 440°C for locality 5. These temperatures can thus be accepted as the highest blocking temperatures of the magnetic constituents involved, probably reflecting presence of pure magnetite and low-titanium TM. Distinct changes in slope of the curves can be detected at 460°C for locality 1, 230°C for locality 2, 250 and 320°C for locality 3, 250°C for locality 5, and 100 and 300°C for locality 4. Those at lower temperatures presumably reflect presence of traces of unoxidized high-titanium TM and/or magnetic pyrrhotite, except for the change at 100°C, which can be ascribed to the presence of quasi-superparamagnetic material of unknown origin.

Summarizing, the IRM studies suggest that the NRM carriers are relatively large grains

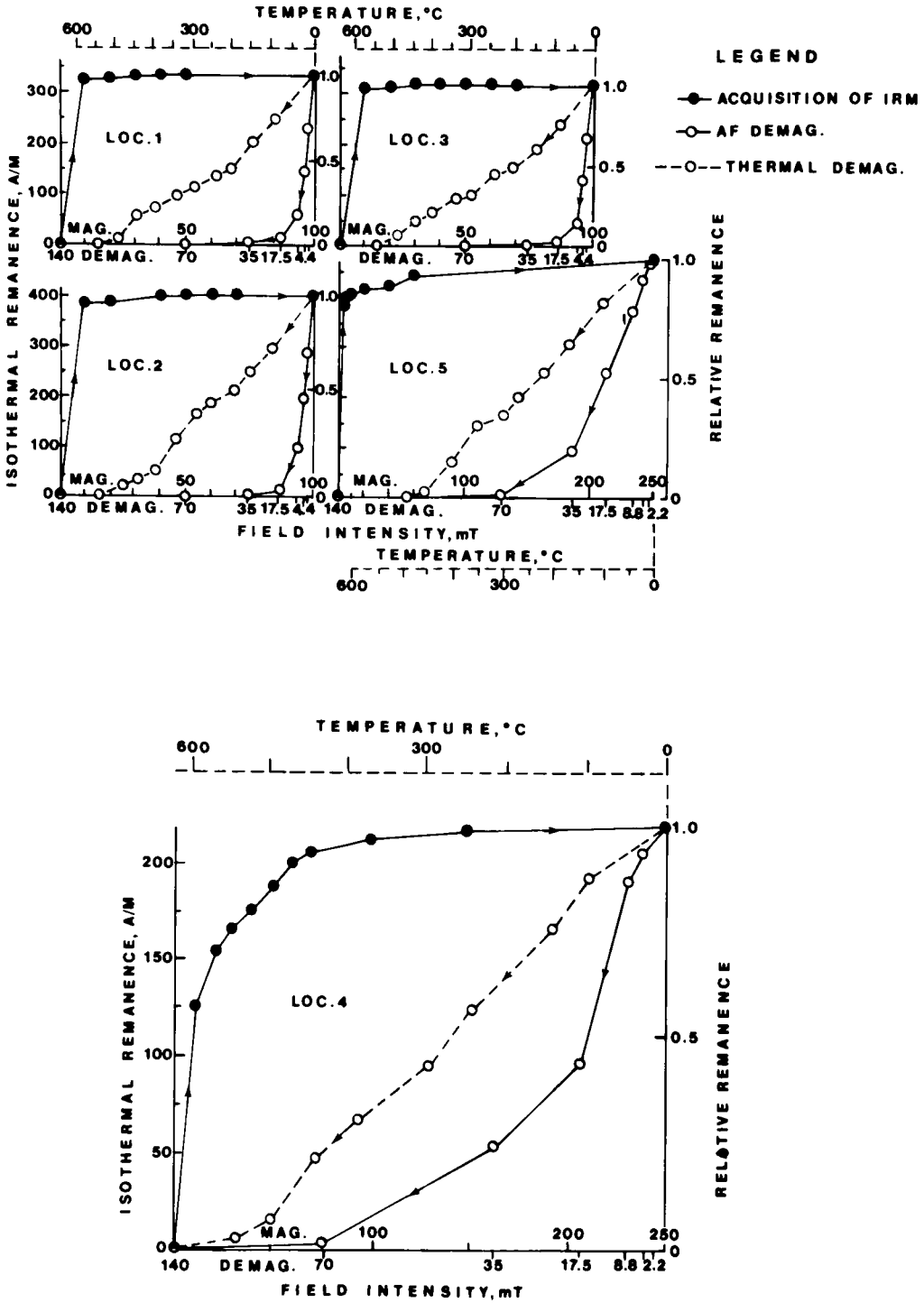

Figure 3. Acquisition and demagnetization of IRM. Ordinates on the left give the magnitude of IRM for the magnetization cycle, ordinates on the right the relative remanence in the demagnetization cycles. The abscissae for the magnetizing fields increase in value to the right and for the demagnetizing alternating peak fields to the left. The abscissae for temperature increase to the left and are shown by dashed lines.

of oxidized TM or magnetite with a group of smaller grains (< 5 μm) at localities 4 and 5 and that magnetic pyrrhotite, if present, plays a minor role as carrier of NRM.

Using a field of 0.047 mT, thermoremanent magnetization (TRM) was imposed on samples used for IRM experiments and on five previously not heated samples referred to as 'fresh' samples and used to monitor phase changes that may have occurred in the 'old' samples as a result of thermal demagnetization of the IRM. The TRM observed was in effect a partial TRM acquired between the heating and room temperatures and measurements were made after the samples had been cooled. The results of those experiments are summarized in Fig. 4. The ordinates on the left side give the TRM magnitudes in units of magnetization present at the beginning of the acquisition process. For 'fresh' samples (locality number circled) the unit is the NRM observed in each sample. For 'old' samples the unit is the residual intensity at the end of the thermal demagnetization cycle of the IRM. While no comparison is made between the absolute values of the TRM acquired by the two groups of samples, its relative values increase at a faster rate in 'old' samples than in 'fresh' samples, except in those from locality 4. This difference is related to the effect of magnetic material generated in 'old' samples by heating during thermal demagnetization of the IRM. Thermal and AF demagnetization of the TRM are recorded on the right-hand ordinates in units of total TRM acquired. The TRM acquisition curves for the first three localities show that, especially in 'fresh' samples, most of the TRM is acquired above 400°C, the blocking temperatures in the temperature range 400–510°C indicating predominance of a titanium-poor TM. In localities 2, 3 and 4 an unstable phase with blocking temperatures above 625°C was found and its instability is ascribed to oxidation of magnetic material during heating in air. Thermal demagnetization of the TRM reveals progressive unblocking of remanence beginning at 440°C. This confirms the presence of titanium-poor TM, but the presence of the second phase with the blocking temperature above 625°C was not detected, since demagnetization was complete at 550°C. A fast-unblocking third phase was, however, indicated in the 100–200°C C interval suggesting the presence of some titanium-rich TM or of some extremely fine grained material in a quasi-superparamagnetic state.

The behaviour of dolerite from locality 4 was different. No TRM was acquired by 'fresh' samples below 400°C and a sudden increase of remanence began at 475°C, increasing at 575°C to almost 60 times its initial value. Thermal demagnetization of the TRM, however, caused unblocking at about 240°C and a complete removal of the TRM at 550°C. The dolerite from locality 5 revealed major blocking temperatures at 550 and 650°C, corresponding to presence of titanohaematite and haematite respectively. The magnitude of of TRM was much lower than at the other localities, an effect which could be attributed to presence of haematite. Finally, as Fig. 4 shows, AF demagnetization was less effective in removing the TRM than heating and cooling in a field-free space. Moreover, the magnetic minerals identified in TRM studies of 'fresh' samples appear to have been well preserved in heated samples of all localities except locality 4, though heating had introduced some changes in behaviour interpreted as being due to generation of haematite or titanohaematite by oxidation as well as due to creation of fresh ferrimagnetic phases which may have contributed to the increase of the TRM. This is confirmed by the curves of TRM acquisition and its thermal demagnetization.

Weak-field volume susceptibility measurements were made on the original fresh samples, as well as on samples subjected to thermal demagnetization of the IRM, and finally on those heated repeatedly for imposition of the TRM. A set of five samples was used in each case to represent each locality (i.e. five samples per locality per case) and the results are summarized in Table 1.

The results show that fresh rock material from localities 4 and 5 has lower susceptibilities

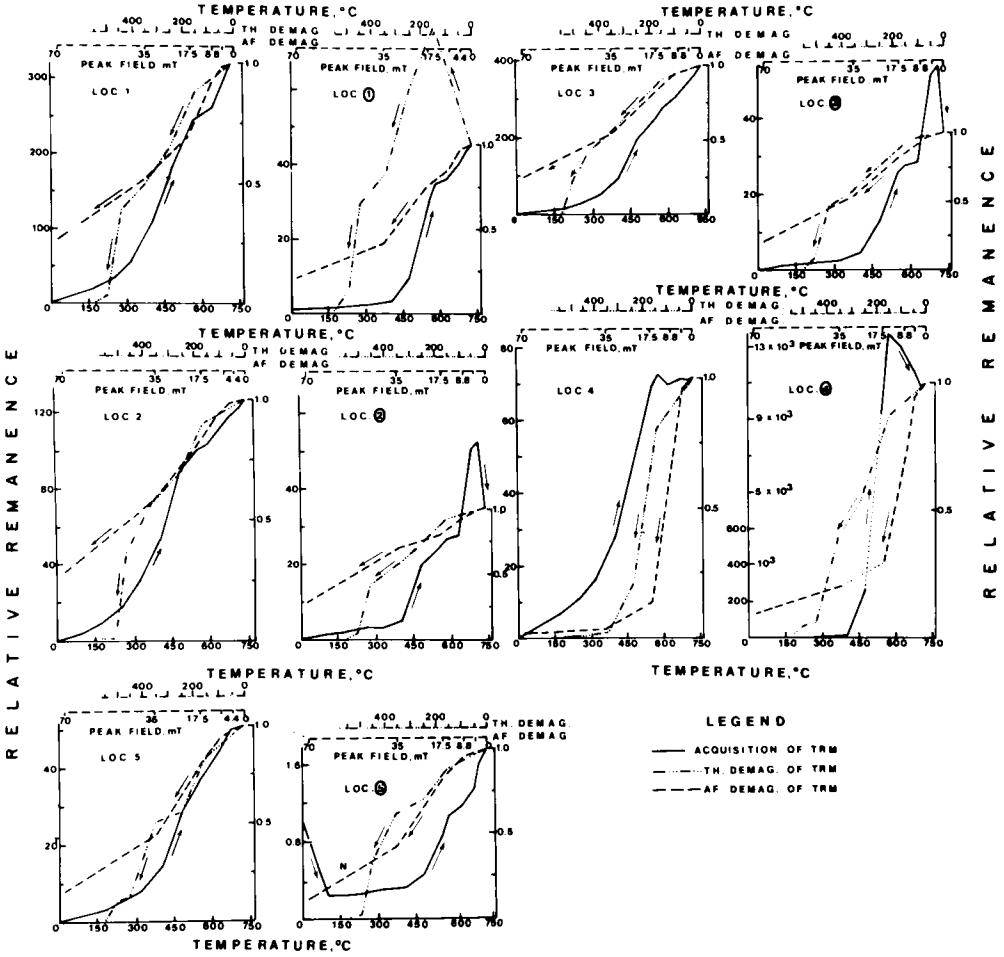

Figure 4. Acquisition of TRM and its AF and thermal demagnetization. For 'fresh' samples the locality number is circled. Demagnetization abscissae are shown above each set of curves and they increase in value to the left. Ordinates give relative remanence in units of initial magnitude. The ordinates on the left give the TRM in units of magnetization present at the beginning of the acquisition process. For 'fresh' samples the unit is the NRM. For 'old' samples the unit is the residual intensity at the end of the thermal demagnetization cycle of the IRM. Thermal and AF demagnetization of the TRM are given on the right-hand ordinates in units of total TRM acquired.

Table 1. Weak-field susceptibilities observed at different stages of experimentation. Units: 10^{-4} SI.

Locality	Original samples	After removal of IRM	After repeated heating
1	391.57 ± 1.07	378.88 ± 5.55	292.17 ± 0.93
2	321.95 ± 4.27	269.67 ± 2.00	242.66 ± 2.12
3	363.29 ± 3.52	293.55 ± 1.45	254.59 ± 1.88
4	23.62 ± 0.78	1148.31 ± 3.44	980.80 ± 1.27
5	185.60 ± 0.45	173.67 ± 1.69	150.29 ± 1.02

than the material at the other localities, suggesting that it is more altered than the material collected from the latter. This is particularly true for locality 4 and agrees with the findings of Johnson & Hall (1978) showing that weak-field susceptibility decreases with increasing low-temperature oxidation. An almost 50-fold increase of susceptibility in samples from this locality, observed after the first heating, indicates that fresh magnetic material has been generated. This agrees with the results obtained by TRM investigations.

To infer the domain structure of constituent magnetic minerals in the dolerite a test proposed by Lowrie & Fuller (1971) was performed. The test utilizes AF demagnetization characteristics of IRM and TRM. In the present case only weak-field TRM was employed. The principal characteristics of this test are as follows: (1) For single domain (SD) carriers the stability of TRM increases with decreasing peak alternating field and the saturation IRM is relatively less stable than the weak-field TRM. (2) For MD carriers, since stability of TRM decreases with decreasing peak field, the saturation IRM is relatively more stable than the weak field TRM. The test thus involves a comparison of stabilities of IRM and TRM obtained from AF demagnetization spectra.

Figs 5 and 6 show the results of progressive AF demagnetization of NRM, IRM and TRM of representative samples of the dolerites from all five localities. Unfortunately, generation of fresh magnetic material on heating samples from locality 4 (Table 1) shows that no significance can be attached to the results of the Lowrie–Fuller (LF) test conducted on material from this locality. The results for the other four localities suggest a predominance of SD grains, because saturation IRM is evidently less resistant to AF demagnetization than than weak-field TRM (Figs 5 and 6a, b, c). In the case of locality 4 predominance of MD material implies merely that most of it was generated by heating in the laboratory (Fig. 6d). The results for localities 1, 2 and 3 are in apparent contradiction to those obtained from IRM acquisition studies and suggesting predominance of MD grains. This contradiction is resolved when it is remembered that the IRM acquisition curve, especially its initial section,

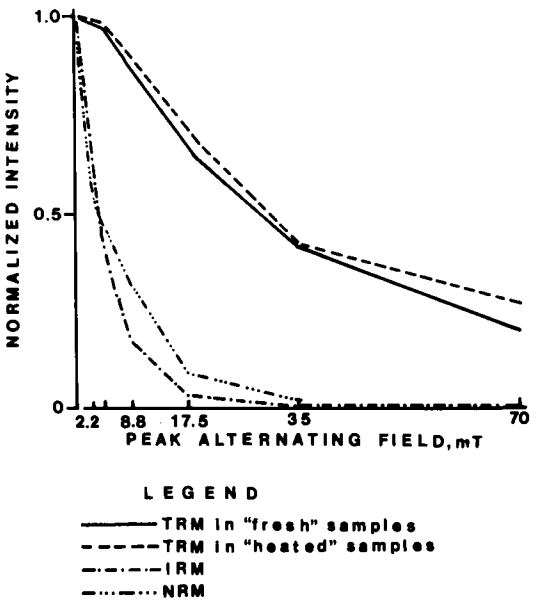

Figure 5. AF demagnetization of various types of remanence in Lowrie–Fuller test of samples of rock from locality 1.

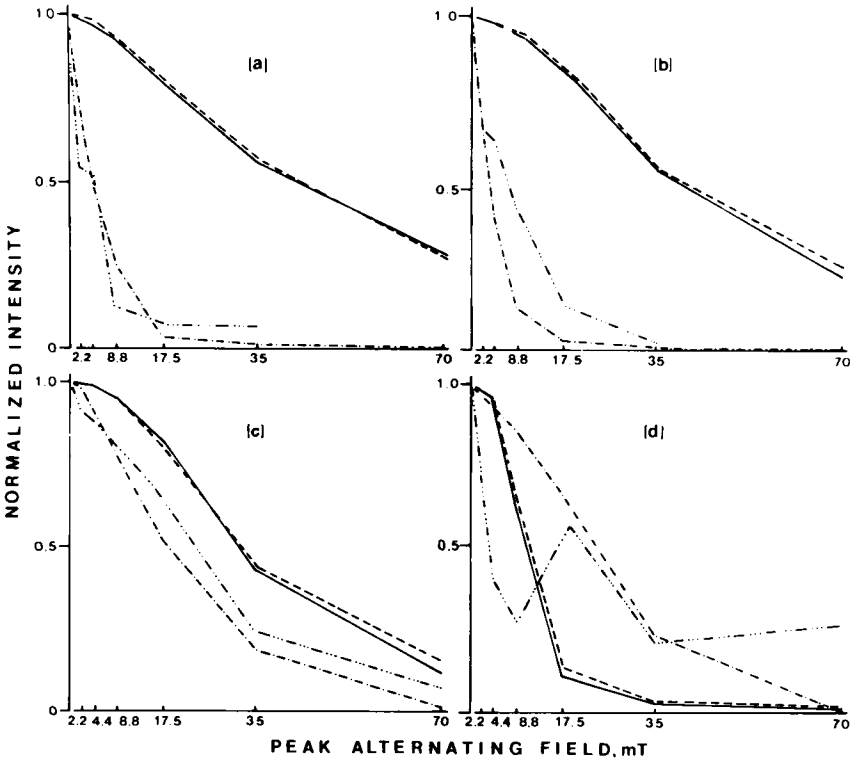

Figure 6. Lowrie–Fuller test of rock samples from localities (a) 2, (b) 3, (c) 5, and (d) 4. Legend as in Fig. 5.

reflects mainly acquisition of remanence by coarse grained oxides, while weak-field TRM resides predominantly in fine grained materials (Verhoogen 1959; Ozima & Ozima 1965). We conclude thus that localities 1, 2 and 3 contain a mixture of SD and MD material, locality 4 contains mostly MD material, while in locality 5 the SD material predominates as shown by the LF test and previous experiments.

It is instructive to compare the AF demagnetization curves of NRM and IRM. In lower peak fields up to 4.4 or 8.8 mT these curves coincide for the material from localities 1, 2, 3 and 5, revealing a comparable stability, but at higher peak fields the slope of the NRM demagnetization curves decreases, tending to that of the TRM curves. When the NRM is normalized to its value after removal of secondary components and is plotted again as full curves beginning at zero demagnetizing peak field (Fig. 7), the coincidence with the corresponding curves of the TRM becomes clear. These curves show clearly that the more stable part of the NRM carried by the dolerites is of a TRM origin.

Figs 5 and 6 show also that the spacing between the individual demagnetizing curves obtained for the dolerites from the first three localities containing, according to the present analysis, a mixture of SD and MD grains, is significantly greater than the spacing between the curves characterized by predominance of SD material. It would appear thus that the spacing between the demagnetizing curves in the LF test can be used as an indicator of the homogeneity of grain size of magnetic constituents. Hence at locality 5, where the curves are very close to each other, the presence of homogeneous SD material is indicated, whereas grain sizes are distinctly variable in the material from localities 1, 2 and 3, suggesting a mixture of SD and MD grains.

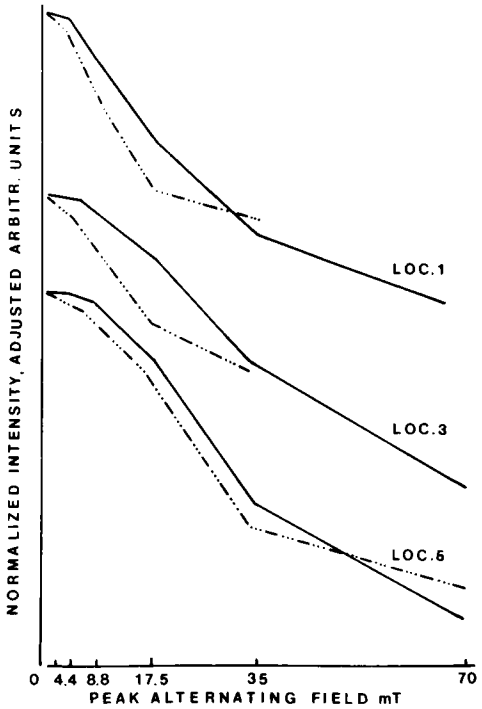

Figure 7. Comparison of AF demagnetization curves of the NRM for localities 1, 3 and 5 (after removal of secondary magnetization) with those of the TRM. Legend as in Fig. 5.

5 Origin of the NRM

The studies described in the preceding sections show that a relatively unaltered titanium-poor TM predominates in the dolerites of the first three localities and a hydrothermally altered TM is present at locality 4 and at the sites of locality 3 designated 3A and, to some extent, at locality 5. The sills contain magnetic minerals ranging widely in grain sizes. Nevertheless, the dolerites from localities 1, 2 and 3 contain a mixture of hard (SD material with high coercivities) and soft (MD material with low coercivities) remanence components involving a bimodal distribution of grain sizes. Microscopic studies suggested that the stable components of remanence was related to small grains present as inclusions in olivines and feldspars, while the unstable components were associated with the large crystals in the groundmass. Occurrence of pyrite-pyrrhotite grains was also observed and that of quasi-superparamagnetic material of unknown origin was surmised. An advanced state of deuteric oxidation, related to abundance of ilmenite lamellae in large TM grains, was associated with SD properties, as at locality 5 where the LF test confirmed predominance of SD grains, while locality 4 was characterized by an advanced stage of hydrothermal alteration. The LF test showed that the stable part of the NRM resided in SD material and comparison of AF demagnetization curves of the NRM with those of the IRM and TRM (Figs 6 and 7) showed that the stable NRM could be related to the TRM process affecting the SD material. This part of the NRM can be thus accepted as the primary remanence imposed at the time of the injection of the sills.

The magnetic phase changes resulting from hydrothermal alteration of the dolerite at locality 4 can be interpreted in terms of replacement of TM by a cation-deficient spinel (CDS) (Ade-Hall, Palmer & Hubbard 1971) which takes the form of titanomaghaemite or

maghaemite. This phase is unstable and breaks down to titanohaematite, haematite and ferrirutile granules. The NRM associated with locality 4 is thus not of primary origin and may have been acquired as a result of some post-formational igneous event. This does not preclude the possibility that it may still have the same direction as the stable NRM carried by the dolerites in localities 1, 2, 3 and 5, but it does not appear to be the original one acquired at the time of the injection of the sill. Using similar arguments it seems legitimate to conclude that the bulk of NRM carried by the hydrothermally altered part of the sill at locality 3 (designated 3A) is also not of primary origin.

6 Palaeomagnetic measurements

Systematic AF demagnetization was applied to representative specimens from block samples derived from each of the five localities using peak fields up to a maximum of 140 mT, but in most cases up to 35 mT. The resulting demagnetization curves are shown in Fig. 8 and typical directional changes in Zijderved (1967) diagrams in Fig. 9. Corresponding results using thermal demagnetization of the NRM up to the temperatures of 530°C are shown in Figs 10 and 11. On the basis of these results the remaining specimens were treated with alternating peak fields 8.8–35 mT or temperatures 300–450°C.

Although some Zijderveld diagrams show that characteristic magnetization becomes apparent at peak fields of 8.8, 17.5 or 35 mT (Fig. 9a, b, c and f), in other cases (Fig. 9d, e and g) the NRM components do not decay linearly toward the origin, suggesting that AF demagnetization was not effective in removing the secondary components. Thermal demagnetization was evidently even less effective, as can be seen from the diagrams in Fig. 11. With a few exceptions, AF and thermal demagnetization lead to similar 'clean' directions with declinations between about 100–200° and negative inclinations ranging from about 30 to 70°. An example of typical directions, those for locality 4, is shown in Fig. 12 and mean directions for all five localities in Fig. 13.

AF demagnetization curves in Fig. 8 reveal a generally low coercivity of the NRM, except in some samples of locality 3 (designated as group 3A), which also have completely different directions from the rest of the samples (Fig. 13). Selected samples at localities 4 and 5 also show much higher coercivities of the NRM (Fig. 8).

Thermal demagnetization curves in Fig. 10 reveal a considerable stability of the NRM against heat in about half of the samples from localities 1, 2 and 4 and in almost all the samples from localities 3 and 5 up to the temperature of about 400°C. In some samples, as in examples given for locality 4, the NRM increases more than twice at temperatures exceeding 400 or 500°C. As discussed in the preceding sections, it is believed that this effect is related to generation by heat of magnetite and/or maghaemite from the iron carbonates and pyrrhotite.

6.1 ANALYSIS OF PALAEOMAGNETIC DIRECTIONS

The final 'clean' directions were selected using Zijderveld diagrams. Despite this procedure some specimens or whole block samples gave either very scattered directions or completely different directions from the majority of the specimens. A systematically different set of directions was obtained in specimens from three sites in locality 3, which have been designated as locality 3A and treated separately in the analysis. Apart from this, a number of specimens from each locality was rejected from the analysis using acceptable rejection criteria relating to inadequate number of specimens per site, misorientation *in situ* or during processing, etc.

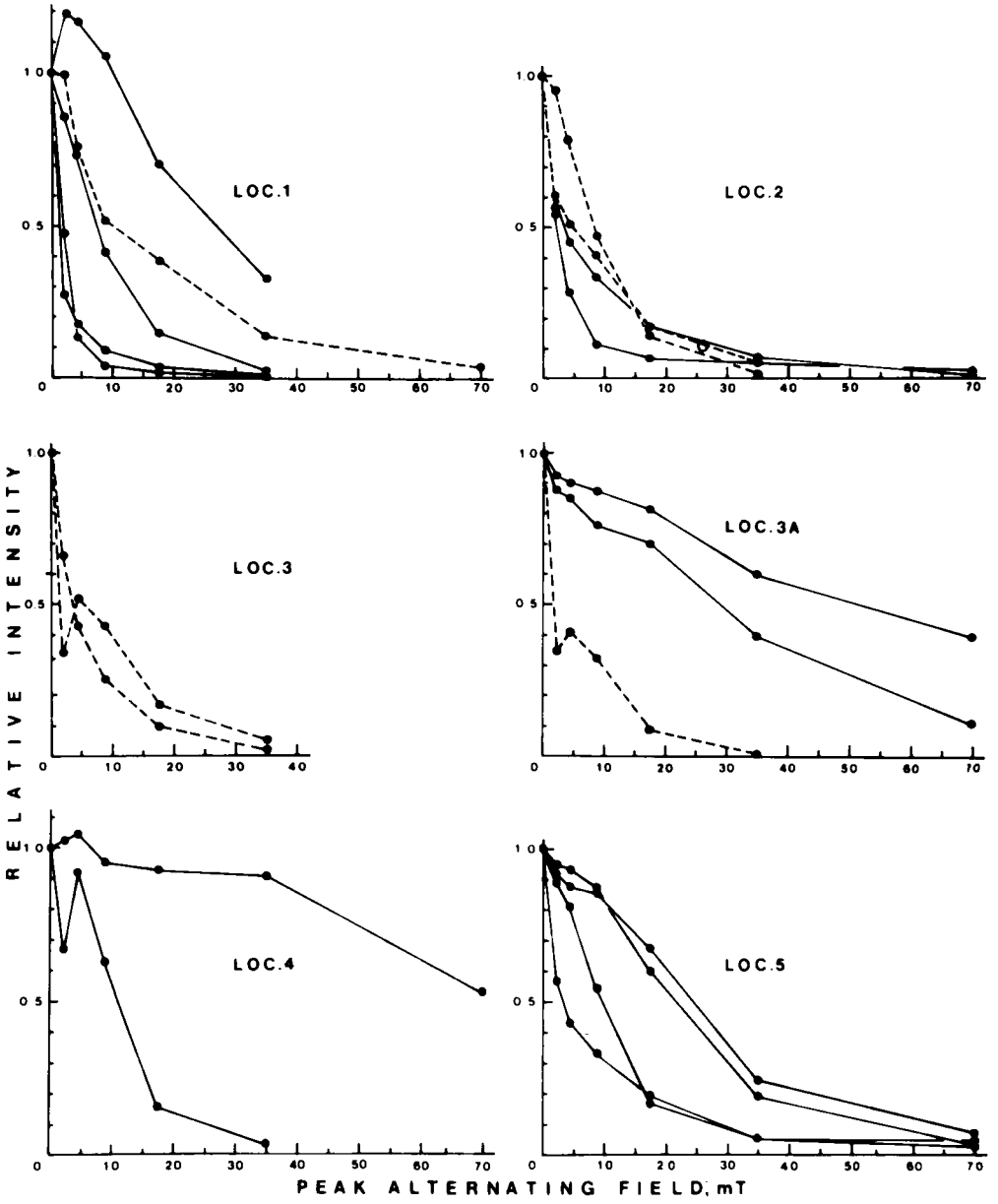

Figure 8. AF demagnetization spectra. The curves representing an average for four or five different specimens are shown by dashed lines.

Using the final selection of samples, statistical analysis was performed the results of which are summarized in the left-hand portion of Table 2. Clearly, all mean directions are similar, except that for locality 3A, which is totally different. Apart from 3A, the mean directions for standard localities show a small scatter, particularly after a further selection was carried out for locality 2, yielding reasonably tightly grouped directions. The average directions for four localities (excluding the whole of locality 3) and for five localities, when locality 3 is included, are given at the bottom of the table.

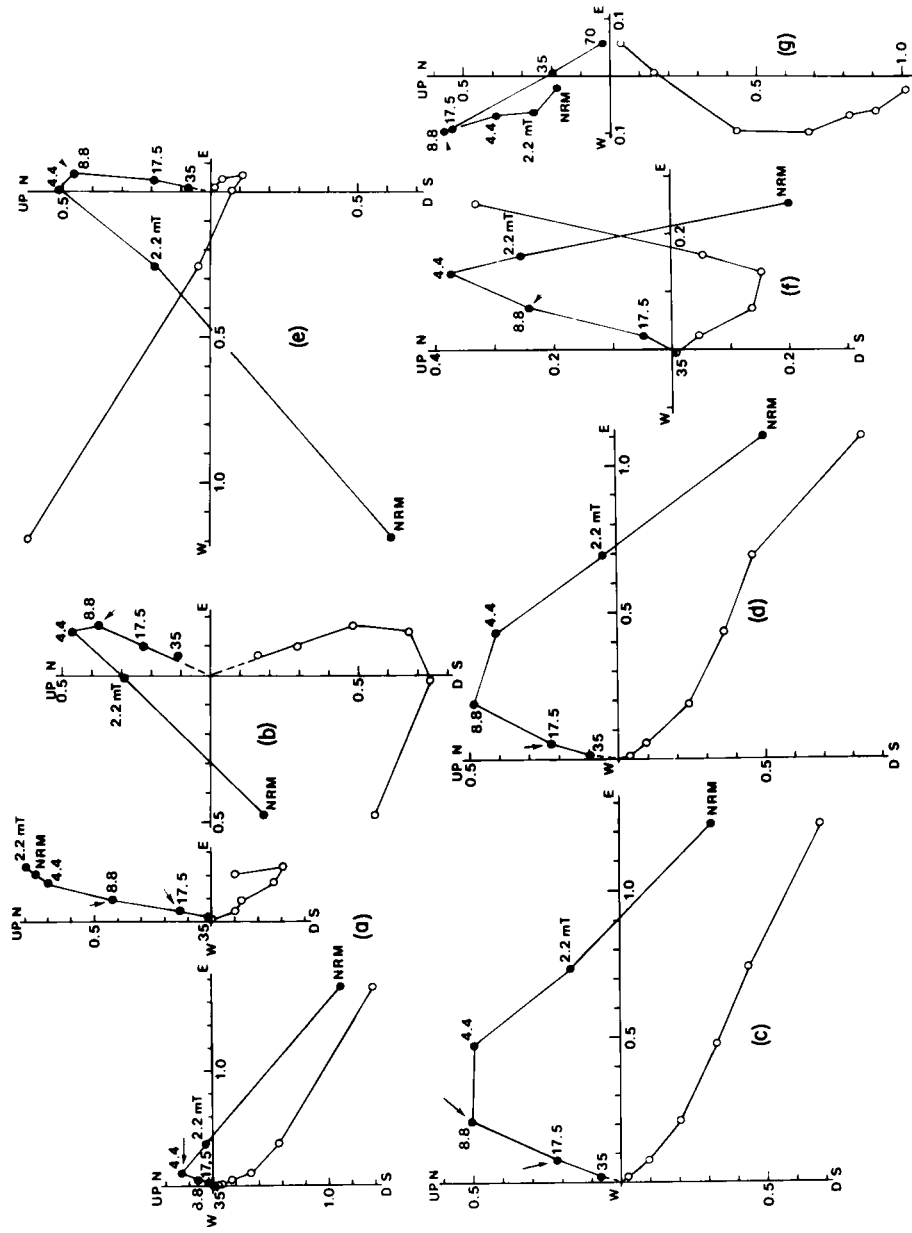

Figure 9. Zijderveld diagrams showing directional changes during AF demagnetization. The points at which the characteristic magnetization becomes apparent are indicated by an arrow: (a) and (b) locality 1, (c) and (d) locality 2, (e) locality 3, (f) locality 4 and (g) locality 5. Units: A m^{-1}. Peak alternating fields in mT.

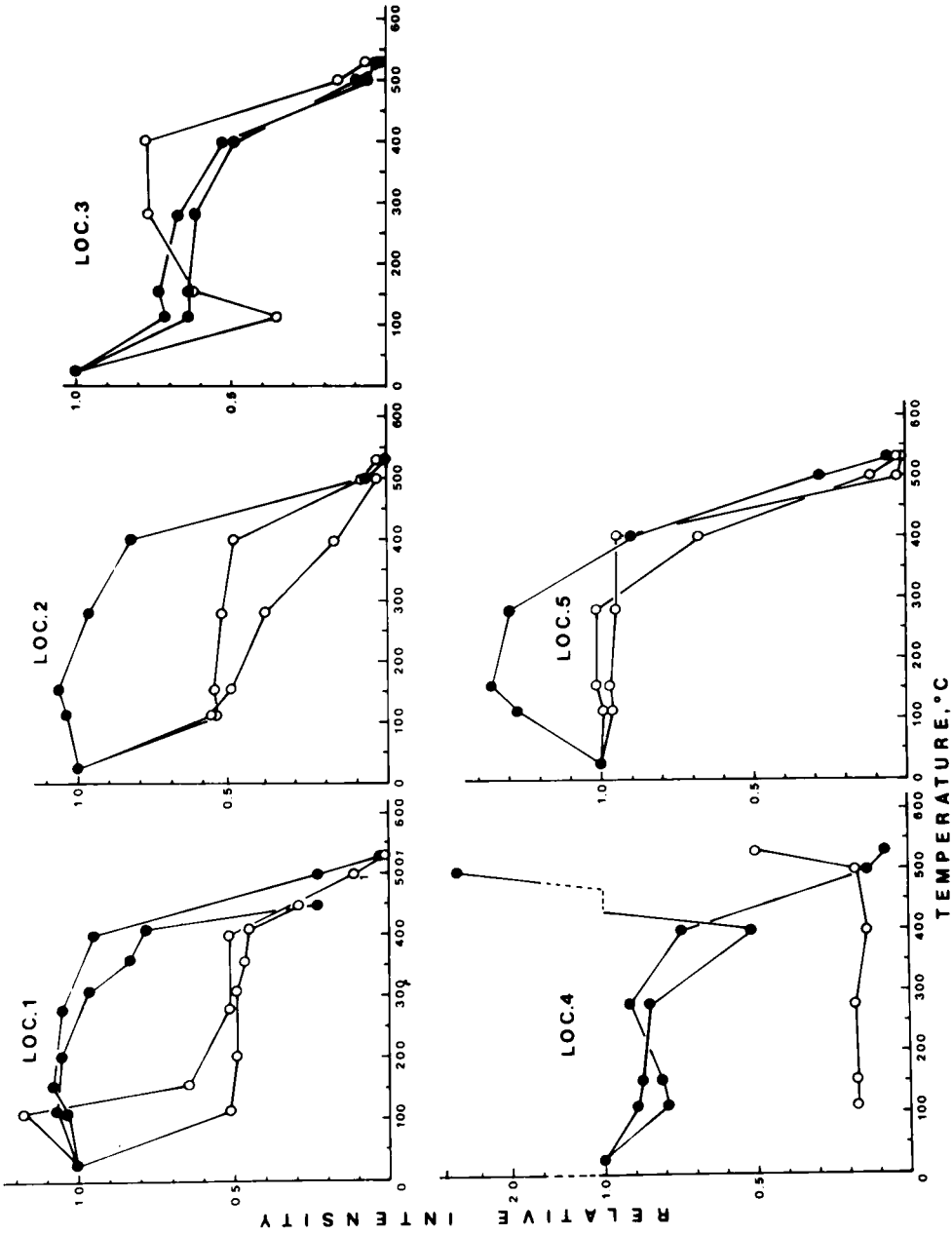

Figure 10. Thermal demagnetization of representative samples from all five localities.

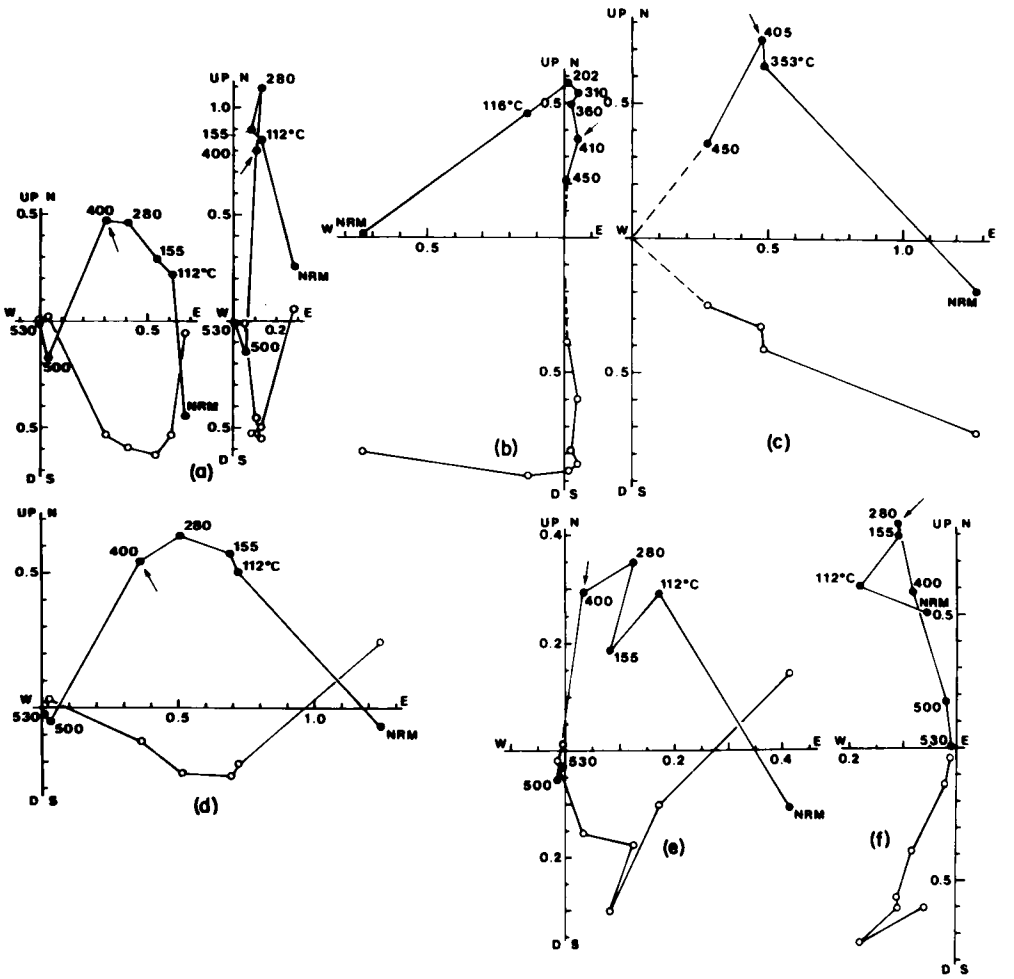

Figure 11. Zijderveld diagrams showing directional changes during thermal demagnetization: (a) and (b) locality 1, (c) locality 2, (d) locality 3, (e) locality 4 and (f) locality 5. Units: A m^{-1}. Temperatures in °C.

6.2 LEAST SQUARES ANALYSIS OF DEMAGNETIZATION DATA

To assess the validity of the analysis described above, a least squares analysis of step demagnetization data was performed, aimed at separating the multicomponent phases. The method, originally developed by Stupavsky & Symons (1978), has already been used in the analysis of palaeomagnetic data from Spitsbergen dolerite dykes (Vincenz *et al.* 1981). The method assumes that the AF demagnetization process can be described by mathematical models according to which the direction of each component remains constant as its intensity decays exponentially during demagnetization. The observed intensity vectors are tested for best fit to several possible models, comprising one, two or three components of different direction, magnitude and stability. The statistical significance of each model is tested for a minimum of five demagnetizing steps. Normally, the analysis is not suitable for thermal demagnetization data, but, as found by Vincenz *et al.* (1981), it worked well with Spitsbergen dolerites and was also applied successfully in the present case.

Unfortunately, not all the dolerite specimens investigated had been taken through five or more demagnetizing steps and hence the number of specimens subjected to this analysis had to be smaller than the number used in the conventional analysis described in the

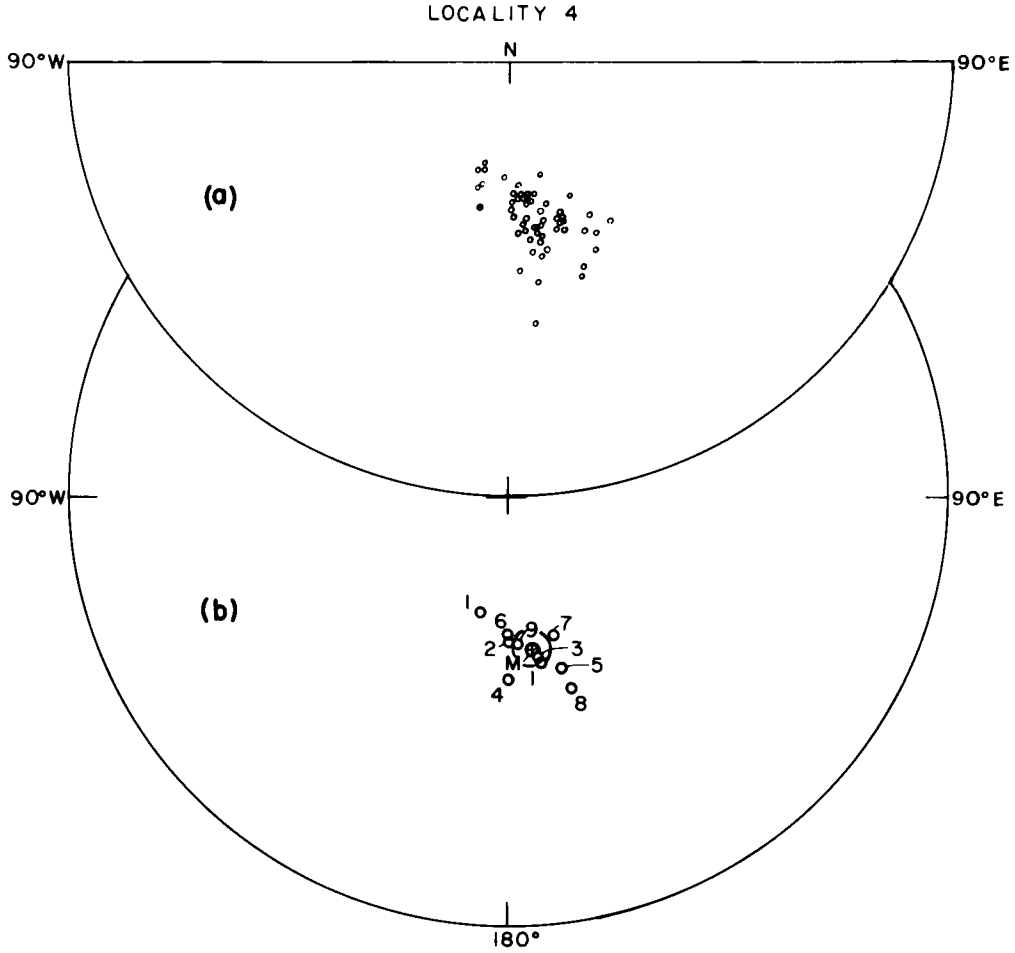

Figure 12. 'Clean' directions of magnetization for locality 4: (a) directions of individual specimens, (b) directions of 10 sites and mean direction (M) for 10 sites together with its 95 per cent circle of confidence.

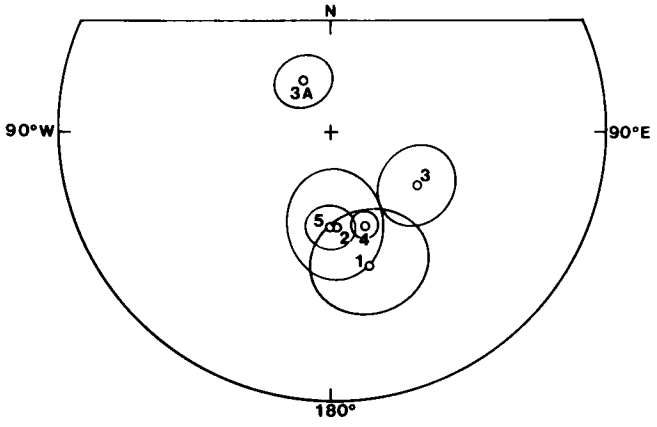

Figure 13. Mean directions of magnetization with their 95 per cent confidence circles for all five localities after AF and thermal demagnetization. The direction derived from the hydrothermally altered part of locality 3, designated 3A, is given separately.

Table 2. Mean directions and statistics after AF and thermal demagnetization.

		Conventional analysis					Least squares analysis				
Locality	N	n	D	I	α_{95}	k	n	D	I	α_{95}	k
1	8 (47)	7 (36)	163.5	−47.8	16.3	14.7	8 (37)	169.4	−49.8	11.3	24.8
2	9 (50)	6 (38)	177.5	−60.7	14.9	21.2	8 (23)	171.8	−63.7	12.4	20.9
3	6 (42)	6 (40)	122.5	−59.2	12.5	29.8	6 (20)	134.3	−59.5	9.9	46.9
3A	4 (28)	3 (25)	333.7	−72.5	8.4	218.1	2 (8)	325.0	61.1	+18.1	193.2
4	13 (75)	10 (57)	170.6	−59.9	3.9	155.1	6 (9)	149.3	−67.4	6.6	105.0
5	11 (77)	10 (69)	178.4	−61.9	7.3	44.3	5 (7)	184.0	−64.9	6.8	127.9
Mean*		4	171.5	−57.7	8.6	114.7	4	169.2	−61.9	11.5	64.7
Mean†		5	162.6	−59.5	12.4	38.9	5	161.9	−62.2	11.0	49.1
Mean‡		6	–	–	–	–	6	159.0	−62.2	9.0	55.7

N is the number of block samples collected and n the number of block samples used in statistical analysis; the figures in parentheses give the total number of specimens in each case; D is the mean declination, I the mean inclination, α_{95} the radius of 95 per cent confidence circle and k an estimate of the precision parameter (Fisher 1953). * localities 3 and 3A excluded; † locality 3A excluded; ‡ all six localities; + no statistical significance can be assigned to this direction based on the mean of only two sites, nevertheless derived from eight specimens.

preceding section. The results of the least squares analysis are summarized in the right-hand portion of Table 2, where they are compared with corresponding results obtained using the conventional procedure.

Except for locality 4 both analyses yield very similar mean directions, but least squares analysis gives on the whole slightly better statistical parameters. An interesting result is obtained for group 3A of locality 3, which now yields a mean direction similar to those in the other localities, except that the magnetization is normal, giving on reversing $D = 145.0°$, $I = -61.1°$. Unfortunately, only two sites yielded significant results and therefore the mean quoted has questionable statistical significance. The value of this result cannot, nevertheless, be overlooked and it is used in obtaining the mean direction for the nominal six localities, since the location of group 3A sites is away from the other locality 3 sites and they can thus be considered as a separate locality 3A.

The mean directions for four, five or six localities (using least squares results only) are given at the bottom of Table 2. It is noteworthy that the statistical parameters for the mean of four localities are better in the case of conventional analysis than for the least squares analysis, but otherwise least squares analysis gives results with a higher statistical significance.

A final comparison between the two methods of analysis is made in Table 3 which lists in

Table 3. Summary of the results.

Localities	n	D	I	α_{95}	k	ϕ'	λ'	δp,	δm	Polarity
Conventional analysis										
1, 2, 4, 5	4	171.5	−57.7	8.6	114.7	208.4	50.1	9.3,	12.6	+
1, 2, 3, 4, 5	5	162.6	−59.5	12.4	38.9	219.9	51.6	14.0,	18.6	+
Least squares analysis										
1, 2, 4, 5	4	169.2	−61.9	11.5	64.7	212.6	56.4	13.8,	17.8	+
1, 2, 3, 4, 5	5	161.9	−62.2	11.0	49.1	221.4	54.6	13.3,	17.1	+
1, 2, 3, 3A, 4, 5	6	159.0	−62.2	9.0	55.7	225.0	54.3	10.9,	14.0	±

ϕ' and λ' are the longitude and latitude of the palaeomagnetic poles in the northern hemisphere; δp, δm are the semi-axes of the 95 per cent oval of confidence; + denotes reversed and ± mixed polarity of the poles; other symbols as in Table 2.

addition to the mean directions and associated statistics also the pole positions obtained from these directions. There is no significant difference between these pole positions.

7 Discussion

One of the aims of this investigation has been to obtain results for late Mesozoic dolerites outside the zone affected by the early Tertiary orogeny. This aim has been accomplished, but microscopic and rock magnetic studies showed that although the 'clean' NRM in rock from localities 1, 2, 3 and 5 was shown to be of primary origin, the NRM at locality 4 and the part of locality 3 designated 3A was secondary. There is no problem in accepting the directions at locality 4, which are very similar to those at other localities and can be ascribed to contemporaneous metasomatism, the mean direction not reflecting any significant changes in geomagnetic field direction. In the case of group 3A conventional analysis produced in the majority of samples a very stable mean direction with $D = 333.7°$, $I = -72.5°$. and in two rejected samples a direction similar to the prevalent direction with $D = 102°$ and $I = -52°$. Least squares analysis revealed presence of another component with normal direction $D = 325.1°$, $I = 61.1°$ (Table 2). It would appear that late Mesozoic metasomatism took the form of multiple localized discrete events, some of which occurred during a change in the direction of the geomagnetic field, reflected by the several NRM components uncovered by the least squares analysis.

The fact that almost all data give reversed directions indicates that the sills were injected during a field reversal event. According to recent information this event would correspond to the Valle del Mis and Quero–Schievenin reversals found in limestones in Southern Alps (VandenBerg & Wonders 1980) and placed respectively in late Albian and early Cenomanian (Lowrie, Channell & Alvarez 1980), i.e. within the 8 Myr period centred on 100 Myr BP. The normal component found in group 3A may correspond to the beginning of change of the field direction back to normal.

The statistically best pole position, computed for six localities using least squares data, is compared in Fig. 14 with three pole positions derived from other late Mesozoic igneous units on Svalbard. These poles were obtained from the Hornsund dolerite dykes of Wedel–Jarlsberg Land within the Tertiary orogenic belt (longitude 222.6°, latitude 69.5°N, Vincenz *et al.* 1981), Sörlifjell lavas (longitude 235°, latitude 75°N, Sandal & Halvorsen 1973) and a dolerite sill of Lomfjord (longitude 210°, latitude 61°N, Briseid & Halvorsen 1974), the latter two outside the orogenic zone. The position of mean pole at 221.7° and 65.2°N with $\alpha_{95} = 12.3°$ and $k = 65.6$ is also shown in Fig. 14. The positions of the mean late Mesozoic Eurasian and North American poles are shown for comparison (Morel & Irving 1981). The results are now quite conclusive, showing that the late Mesozoic poles for Svalbard are distinct from both North American and Eurasian Cretaceous poles.

The palaeolatitudes of the four sampling regions on Spitsbergen are given in Table 4. The table reveals some differences between the palaeolatitudes of the sampling areas in the eastern part of the island containing the dolerite sills at Agardhbukta and Lomfjord and those in the western part containing the Hornsund dolerite dykes and the Sörlifjell volcano in the north (Fig. 1b), but there is no geological evidence for relative displacement between the eastern and western parts of the island since late Mesozoic. Although Harland *et al.* (1974) suggested a possible up to 1000 km sinistral north–south stike-slip movement along the Billefjorden fault (Fig. 1b) in the late Devonian, continuity of Mesozoic sediments across the fault indicates no such movements along the fault in the Mesozoic. Moreover, recent palaeomagnetic studies reveal no significant differences in NRM directions in Permo-Carboniferous sediments on both sides of the fault (Jeleńska & Vincenz, in preparation). The

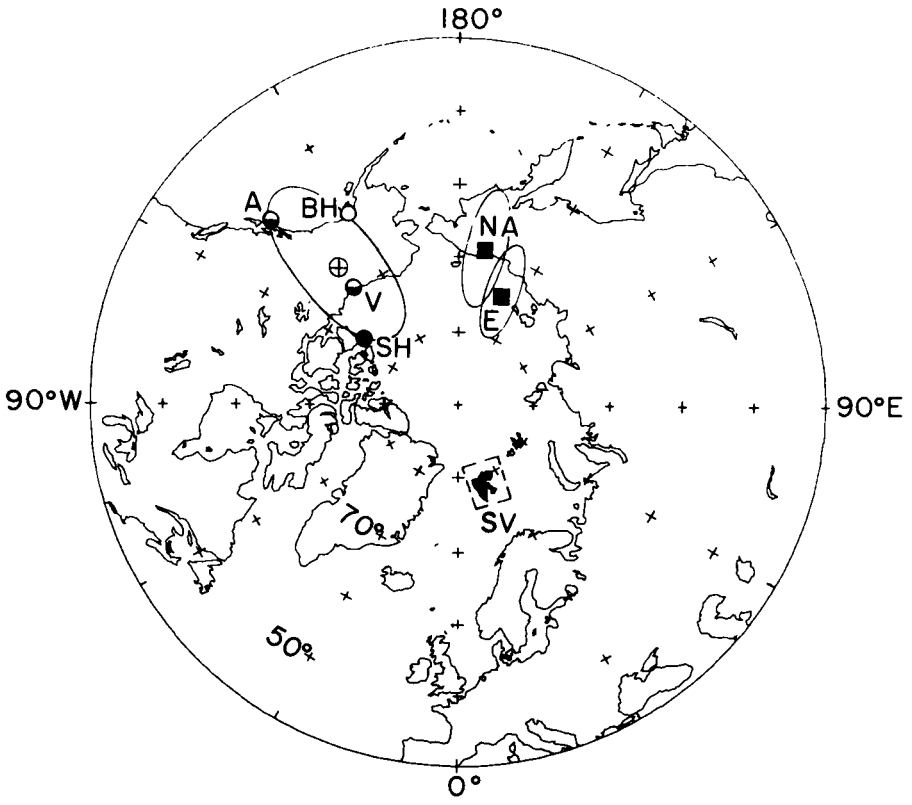

Figure 14. Late Mesozoic palaeomagnetic poles for Svalbard. Spitsbergen dolerites and lavas: normal polarity, full circles; reversed polarity, open circles; mixed polarity, half-full circles. This study: A, Agardhdalen sills. Other studies: SH, Sandal & Halvorsen (1973); BH, Briseid & Halvorsen (1974); V, Vincenz *et al.* (1981). Mean of four poles: circle with a cross. Full squares: NA, mean Cretaceous pole for North America for the time interval 83–159 Myr BP; E, mean Cretaceous pole for Eurasia for approximately the same time interval (Morel & Irving 1981); SV, Svalbard Archipelago. Ninety-five per cent circles of confidence for mean poles are also shown.

Table 4. Palaeolatitudes of late Mesozoic igneous centres on Spitsbergen.

Name of centre	Palaeopole (Fig. 14)	Inclination	Palaeolatitude
Agardhbukta	A	62.2°	43.5° N
Lomfjord	BH	68.0°	51.1° N
Sörlifjell	SH	77.0°	65.2° N
Hornsund	V	72.3°	57.4° N

scatter in palaeolatitudes listed in Table 4 thus probably reflects different ages of magnetization in similar rock units.

Mean palaeolatitude computed from the data in Table 4 and incorporating a correction to obtain its unbiased estimate and variance (Cox & Gordon 1984) is 57.0 ± 8.5°N, suggesting that during the late Mesozoic Svalbard was about 24° south of its present position. The fact that the Mesozoic palaeopoles for Svalbard are distinct from those obtained from North American and Eurasian data leads to the conclusion that Svalbard existed at the time as a

separate tectonic entity. In a recent study of plate tectonics of the Arctic Basin Savostin & Karasik (1981) suggested that present-day Svalbard could be looked upon as a microplate. While recent earthquake studies suggest that Svalbard is not separated from Eurasia by a major plate boundary (Mitchell *et al.* 1979; Chan & Mitchell 1984), our studies provide grounds for believing that such a boundary existed in the past.

8 Conclusions

The dolerite sills of Agardhadalen situated on the east coast of Vestspitsbergen are reversely magnetized and yield palaeomagnetic pole positions similar to those obtained from other late Mesozoic intrusives of Svalbard. The Mesozoic palaeomagnetic poles for Svalbard are distinct from the corresponding North American and Eurasian poles. The results suggest that during the late Mesozoic Svalbard existed as a separate microplate more or less detached from both Eurasia and North America. The fact that the Cretaceous North American palaeopole lies west of the Svalbard pole and both lie east of the Eurasian pole suggests that North America and Svalbard have separated from Eurasia in post-Cretaceous times.

Acknowledgments

We are indebted to J. E. Kohsmann, formerly of Saint Louis University and now with Texaco Inc., Houston, Texas and to J. Jeleński of the Polish Academy of Sciences, Warsaw for assistance in collection of samples. We also thank the referees for their helpful comments and suggestions which guided us in revising the original version of the paper.

This reseach was supported by the Division of Polar Programs, National Science Foundation, Grant DPP77-27241.

References

Ade-Hall, J. M., Kahn, M. A., Dagley, P. & Wilson, R. L., 1968. A detailed opaque petrological and magnetic investigation of a single Tertiary lava flow from Skye, Scotland, I., Iron and titanium oxide petrology, *Geophys. J. R. astr. Soc.*, **16**, 375–388.

Ade-Hall, J. M., Palmer, H. C. & Hubbard, T. P., 1971. The magnetic and opaque petrological response of basalts to regional hydrothermal alteration, *Geophys. J. R. astr. Soc.*, **24**, 137–174.

Birkenmajer, K., 1972. Tertiary history of Spitsbergen and continental drift, *Acta. geol. Pol.*, **22**, 193–218.

Briseid, E. & Halvorsen, E., 1974. The primary magnetic remanence of a dolerite sill from northeast Spitsbergen, *Phys. Earth planet. Int.*, **9**, 45–50.

Burov, J. P., Krasilsakov, A. A. Firsov, L. V. & Klubov, B. A., 1977. The age of Spitsbergen dolerities (from isotopic dating), *Norsk Polar Institutt Arb.* 1975, 101–108.

Chan, W. W. & Mitchell, B. J., 1984. Intraplate earthquakes in Northern Svalbard, *Tectonophys.*, in press.

Cox, A. & Gordon, R. G., 1984. Paleolatitudes determined from paleomagnetic data from vertical cores, *Rev. Geophys. Space. Phys.*, **22**, 47–72.

Dankers, P., 1981. Relationships between media destructive field and remanent coercive forces for dispersed natural magnetite, titanomagnetite and haematite, *Geophys. J. R. astr. Soc.*, **64**, 447–461.

Day, R., 1977. TRM and its variation with grain size: a review, *J. Geomagn. Geoelect., Kyoto*, **29**, 233–266.

Fisher, R. A., 1953. Dispersion on a sphere, *Proc. R. Soc. A*, **217**, 295–305.

Harland, W. B., 1969. Contribution of Spitsbergen to understanding of tectonic evolution of North Atlantic region, in *North Atlantic Geology and Continental Drift*, ed. Kay, M., *Mem. Am. Ass. Petrol. Geol.*, **12**, 817–851.

Harland, W. B., Cutbill, J. L., Friend, P. F., Gobbett, D. J., Holliday, D. W., Maton, P. I., Parker, J. R. & Wallis, R. H., 1974. The Billefjorden fault zone, Spitsbergen, *Norsk Polarinstitutt, Skrifter Nr 161*, 1–72.

Jeleńska, M., Kądziałko-Hofmokl, M., Kruczyk, J. & Vincenz, S. A., 1978–79. Thermomagnetic properties of some diabase dikes of South Spitsbergen, *Pure appl. Geophys.*, **117**, 784–794.

Johnson, H. P., & Hall, J. M., 1978. A detailed rock magnetic and opaque mineralogy study of the basalts from the Nazca plate, *Geophys. J. R. astr. Soc.*, **52**, 45–62.

Johnson, H. P. & Melson, W. G., 1977. Electron microprobe analyses of some titanomagnetite grains from hole 395A, in *Init. rep. Deep Sea drill. Proj.*, **45**, eds Melson, W. G. & Rabinowitz, P. D., US Government Printing Office, Washington, DC.

Lowrie, W., Channell, J. E. T. & Alvarez, W., 1980. A review of magnetic stratigraphy investigations in Cretaceous pelagic carbonate rocks, *J. geophys. Res.*, **85**, B7, 3597–3605.

Lowrie, W. & Fuller, M., 1971. On the alternating-field demagnetization characteristics of multidomain thermoremanence in magnetite, *J. geophys. Res.*, **76**, 6339–6349.

Marshall, M. & Cox, A., 1972. Magnetic changes in pillow basalt due to sea floor weathering, *J. geophys. Res.*, **77**, 6459–6469.

Mitchell, B. J., Zollweg, J. E., Kohsmann, J. J., Cheng, C. C. & Haug, E. J., 1979. Intra-plate earthquakes in Svalbard Archipelago, *J. geophys. Res.*, **84**, B10, 5620–5626.

Morel, P. & Irving, E., 1981. Paleomagnetism and the evolution of Pangea, *J. geophys. Res.*, **86**, B3, 1858–1872.

Ozima, M. & Ozima, M., 1965. Origin of thermoremanent magnetization, *J. geophys. Res.*, **70**, 1363–1369.

Ryall, P. J. C. & Hall, J. M., 1980. Iron loss in titanomagnetites during low-temperature oxidation, *J. Geomagn. Geoelect., Kyoto*, **32**, 661–669.

Sandal, S. T. & Halvorsen, E., 1973. Late Mesozoic palaeomagnetism from Spitsbergen; implications for continental drift in the Arctic, *Phys. Earth planet. Int.*, **7**, 125–132.

Savostin, L. A. & Karasik, A. M., 1981. Recent plate tectonics of the Arctic Basin and of the North-eastern Asia, *Tectonophys.*, **74**, 111–145.

Schwarz, E. J., 1967. Dependence of magnetic properties on the thermal history of natural polycrystalline pyrrhotite, $Fe_{0.89}S$, *J. Geomagn. Geolect., Kyoto*, **19**, 91–101.

Schwarz, E. J., 1968. Magnetic phases in natural pyrrhotite $Fe_{0.89}S$ and $Fe_{0.91}S$, *J. Geomag. Geoelect., Kyoto*, **20**, 67–74.

Schwarz, E. J., 1975. Magnetic properties of pyrrhotite and their use in applied geology and geophysics, *Pap. geol. Surv. Can. Dept Energy, Mines Resources*, Ottawa, 74–79.

Soffel, H., 1971. The single-domain-multi-domain transition in natural intermediate titanomagnetites, *Z. Geophys.*, **37**, 451–470.

Stupavsky, M. & Symons, D. T. A., 1978. Separation of magnetic components from AF step demagnetization data by least squares computer methods, *J. geophys. Res.*, **83**, 4925–4931.

Tyrell, G. W. & Sandford, K. S., 1933. Geology and petrology of the dolerites of Spitsbergen, *Proc. R. Soc. Edinb.*, **53**, 284–321.

VandenBerg, J. & Wonders, A. A. H., 1980. Paleomagnetism of late Mesozoic pelagic limestones from the Southern Alps, *J. geophys. Res.*, **85**, B7, 3623–3627.

Verhoogen, J., 1959. The origin of thermoremanent magnetization, *J. geophys. Res.*, **64**, 2441–2449.

Vincenz, S. A., Jeleńska, M., Birkenmajer, K., Cossack, D., Kądziałko-Hofmokl, M. Kruczyk, J. & Duda, S. J., 1981. Palaeomagnetism of some late Mesozoic dolerite dykes of South Spitsbergen, *Geophys. J. R. astr. Soc.*, **67**, 599–614.

Wilson, R. L., Haggerty, S. E. & Watkins, N. D., 1968. Variation of palaeomagnetic stability and other parameters in a vertical traverse in a single Icelandic lava, *Geophys. J. R. astr. Soc.*, **16**, 79–96.

Wilson, R. L. & Watkins, N. D., 1967. Correlation of petrology and natural magnetic polarity Columbia Plateau basalts, *Geophys. J. R. astr. Soc.*, **12**, 405–424.

Zijderveld, J. D. A., 1967. A. C. demagnetization of rocks: analysis of results, in *Methods of Palaeomagnetism*, eds Collinson, D. W., Creer, K. M. & Runcorn, S. K., *Developments in Solid Earth Geophysics*, **3**, 254–286.